

## Support Information

### Experimental Section

#### General procedures and materials

3,6-di(*tert*-butyl)carbazole and zinc bromide were purchased from Adamas-beta, tetrakis(triphenylphosphine)palladium(0) was purchased from Energy Chemical, 2-(tributylstannyl)pyridine was purchased from Bidepharm, bromine, toluene and acetic acid were purchased from Sinopharm Chemical Reagent Co., Ltd., China. All chemical materials and solvents were not further purified, except those with further notice.

#### 1,8-Dibromo-3,6-di(*tert*-butyl)carbazole

3,6-di(*tert*-butyl)carbazole (8.1 g, 29 mmol) was dissolved in glacial acetic acid (120 mL), and a solution of acetic acid containing bromine (3 mL, 60 mmol) was added at 90 °C, the mixture was stirred in 90 °C for 3.5 h under Ar atmosphere. After cooling to room temperature, the reaction mixture is concentrated and dried, and the residue is washed with NaOH solution to obtain a white solid. (10.2 g, 80.44%): <sup>1</sup>H NMR (400 MHz, DMSO, ppm) δ: 10.89 (br s, 1H), 8.26 (s, 2H), 7.63 (s, 2H), 1.39 (s, 18H).

#### 1,8-Di(pyrid-2'-yl)-3,6-di(*tert*-butyl)carbazole

1,8-dibromo-3,6-di(*tert*-butyl)carbazole (1.53 g, 3.6 mmol), 2-(tributylstannyl)pyridine (4.98 g, 11.4 mmol), tetrakis(triphenylphosphine)palladium(0) (0.2079 g, 0.18 mmol) and anhydrous toluene (10 mL) were added in a double-necked flask and refluxed for 20 h under Ar. After cooling to room temperature, the solvent is evaporated by vacuum, and the crude product is purified by silica gel column chromatography eluting with ethyl acetate/hexane (1:20) to obtain the product as a yellow powder. (1.03 g, 65.8%): <sup>1</sup>H NMR (400 MHz, DMSO, ppm) δ: 13.10 (br s, 1H), 9.00 (dd, 2H, *J* = 4.8, 1.2 Hz), 8.40 (d, 2H, *J* = 1.6 Hz), 8.34 (d, 2H, *J* = 8.4 Hz), 8.15 (d, 2H, *J* = 1.6 Hz), 7.99 (t, 2H, *J* =

15.6 Hz), 7.45-7.42 (m, 2H), 1.51 (s, 18H).

### **Complexes 1 and 2**

To a mixture of 1,8-Di(pyrid-2'-yl)-3,6-di(tert-butyl)carbazole (0.0433 g, 0.1 mmol), zinc bromide (0.0225 g, 0.1 mmol) in 12 mL of acetic acid were reflux 24 h. After cooling to room temperature, yellow needle-like crystals **1** generated on the wall of the bottle. The crystals were picked out, and the rest of the solution was placed open and volatilized for more than ten days, resulting in dark yellow needle-like crystals **2**. Neither crystal had been further purified since it was isolated.

### **Characterization.**

Single-crystal X-ray diffraction (SCXRD) data of both compounds were recorded using Bruker D8 ADVANCE with a graphite-monochromated Mo-K $\alpha$  ( $\lambda = 0.71073 \text{ \AA}$ ) radiation. The structure was solved by the direct method using a SHELXL-97 program. Powder XRD (PXRD) patterns were measured on Rigaku MiniFlex 600 with a Cu-K $\alpha$  ( $\lambda = 1.54184 \text{ \AA}$ ) radiation in the range of  $5^\circ$ – $30^\circ$  at a scan rate of  $2^\circ \text{ min}^{-1}$ . Thermogravimetry analysis (TGA) was carried out using Netzsch STA449F3 thermal system. The samples were heated from 35 to 800 °C with at a rate of  $10^\circ \text{ C min}^{-1}$  under N<sub>2</sub> atmosphere. PL properties, including emission and excitation spectra in solid state at room temperature, were collected on an FLS920 Edinburgh fluorescence spectrometer. In addition, PL quantum efficiency measurements were reported using the same light source with an additional integrating sphere. The dynamics of emission decay were monitored using the time-correlated single-photon counting capability of FLS920 (1024 channels, 50-ns window) with data collection for 10,000 counts. Excitation was provided by an Edinburgh EPL-375 picosecond pulsed diode laser. Ultraviolet-visible (UV-Vis) absorption spectra were obtained using a PerkinElmer LAMBDA 950 UV-Vis spectrophotometer using BaSO<sub>4</sub> powder as a reflectance reference. The absorption spectra were obtained using powders from single crystals. The energy band structures and density of states (DOS) of **1** and **2** were theoretically calculated by using the first-principles plane-wave pseudopotential method with the code CASTEP provided by the software Materials Studio v7.0<sup>1-2</sup>. The generalized

gradient approximation (GGA) functional of Perdew–Burke–Ernzerh (PBE)<sup>3</sup> was employed for the geometry optimization and energy calculation. The precise of the plane wave basis sets was set as 340 eV cutoff energy. The k-point mesh in the Brillouin zone was represented as 1\*1\*1 of the Monkhorst-Pack grid and the ultrasoft pseudopotentials in the reciprocal space was used. The other calculating parameters and convergent criteria were set the default values of the CASTEP code.

**Table S1. Crystal data for compounds 1 and 2.**

	1	2
	(C <sub>30</sub> H <sub>33</sub> N <sub>3</sub> )Zn <sub>2</sub> Br <sub>4</sub> (CH <sub>3</sub> COO) <sub>2</sub> •CH <sub>3</sub> COOH	
Temperature (K)	100	100
Crystal system	orthorhombic	orthorhombic
Space group	P2(1)2(1)2(1)	P2(1)2(1)2(1)
<i>a</i> (Å)	12.9603	12.9576
<i>b</i> (Å)	14.4113	14.4213
<i>c</i> (Å)	22.3844	22.3577
<i>α</i> (deg)	90	90
<i>β</i> (deg)	90	90
<i>γ</i> (deg)	90	90
Volume (Å <sup>3</sup> )	4180.84	4016.31
<i>Z</i>	1	1
$\rho_{\text{calc}}$ (mg m <sup>-3</sup> )	1.6888	1.5961
$\mu$ (mm <sup>-1</sup> )	5.015	5.010
Radiation (Å)	0.71073	0.71073
R <sub>1</sub> <sup>a</sup>	0.0736	0.0761
wR <sub>2</sub> <sup>b</sup>	0.2129	0.2318
GOF	1.020	1.053

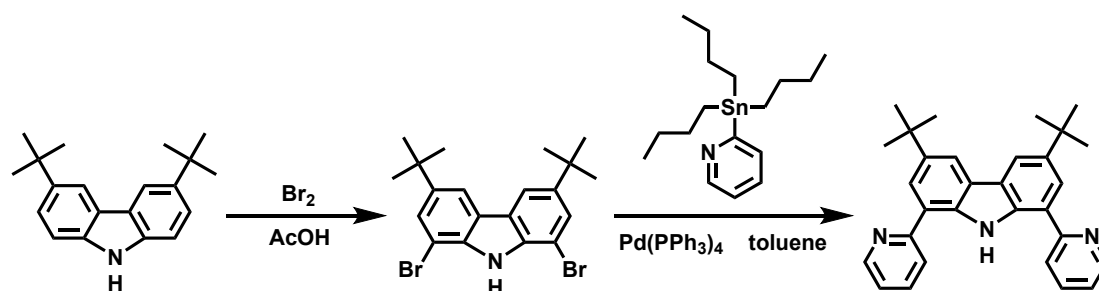


Figure S1. Synthesis route of tBuCarPy ligand.

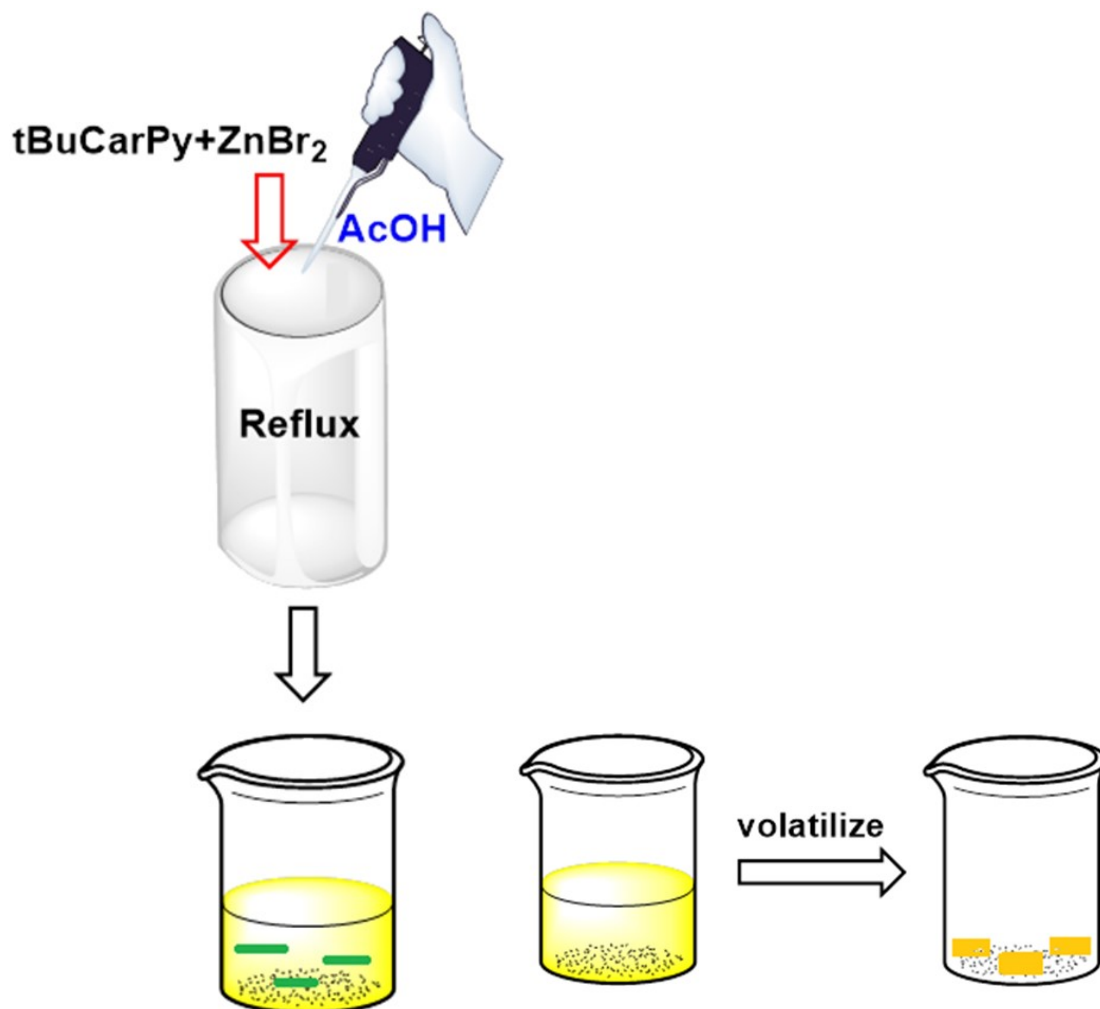


Figure S2. Schematic diagram of synthesis of complexes 1 and 2.

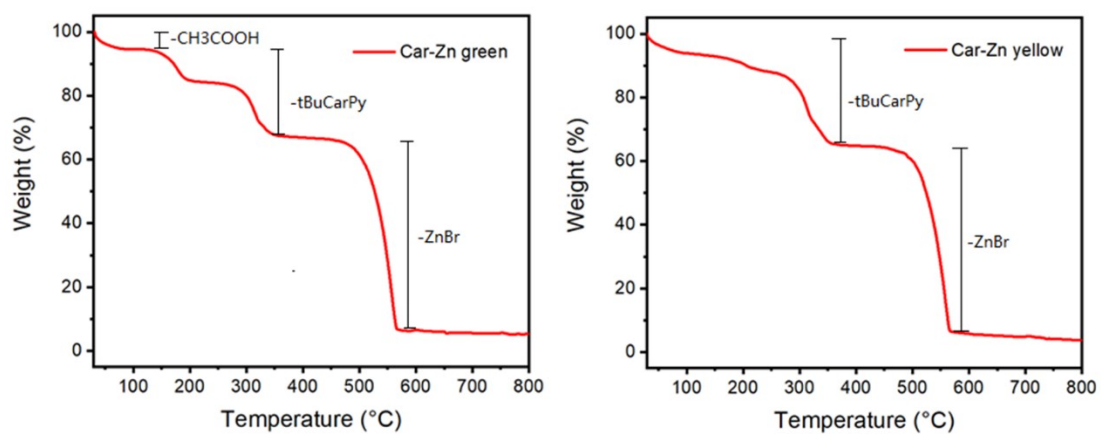
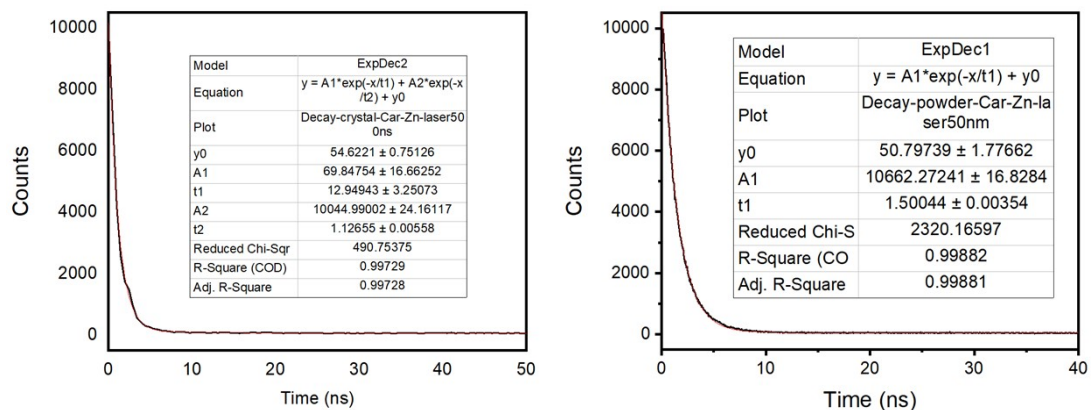
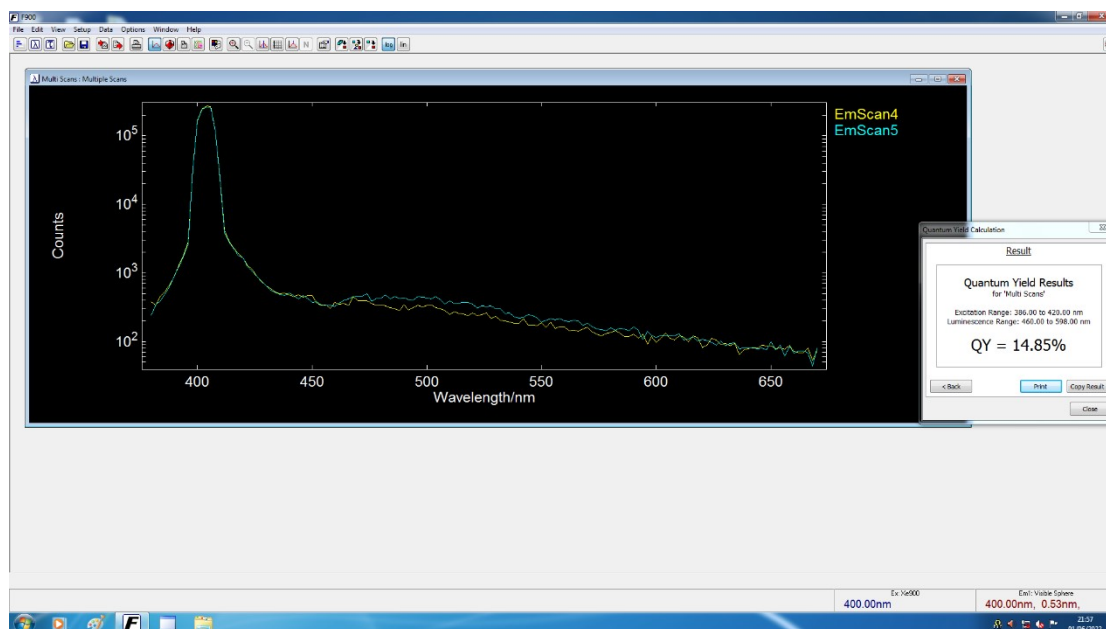


Figure S3. Thermogravimetric curves of complexes 1 and 2.



**Figure S4. The emission decay curves of 1 peaked at 500 nm and 2 peaked at 550 nm.**



**Figure S5. PLQY of complex 1.**

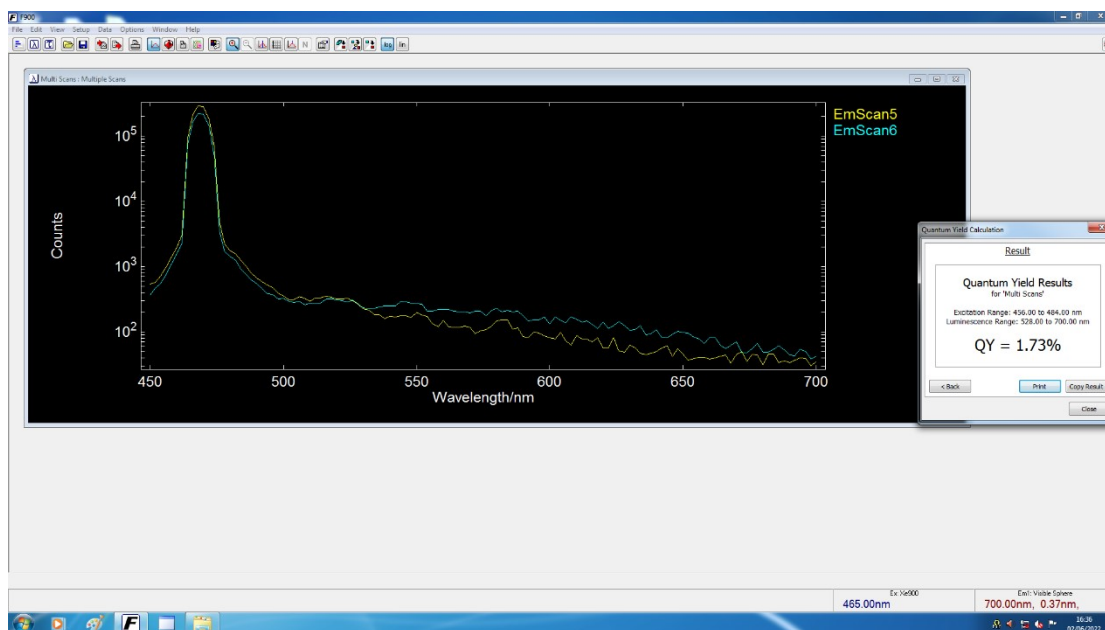


**Figure S6. PLQY of complex 2.**

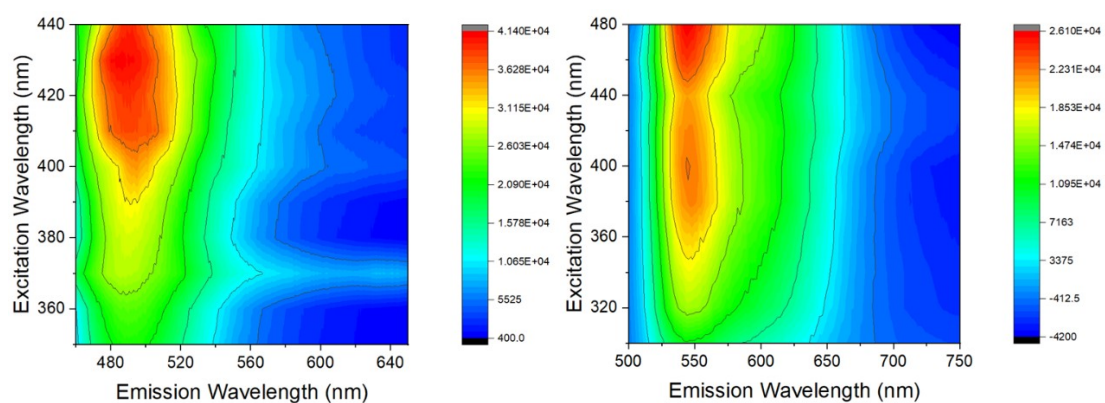


**Figure S7. The 3D PL spectra of 1 and 2 recorded at different excitation wavelengths.**

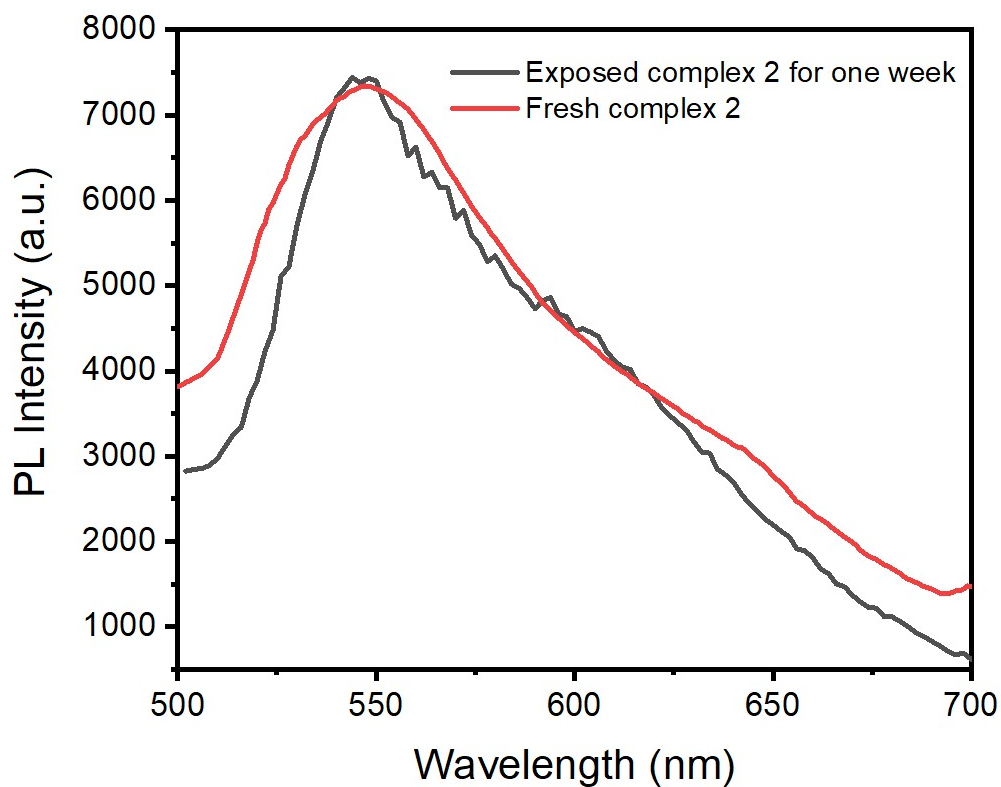


Figure S8. PL spectra of fresh complex 2 and complex 2 after one week of exposure to air.

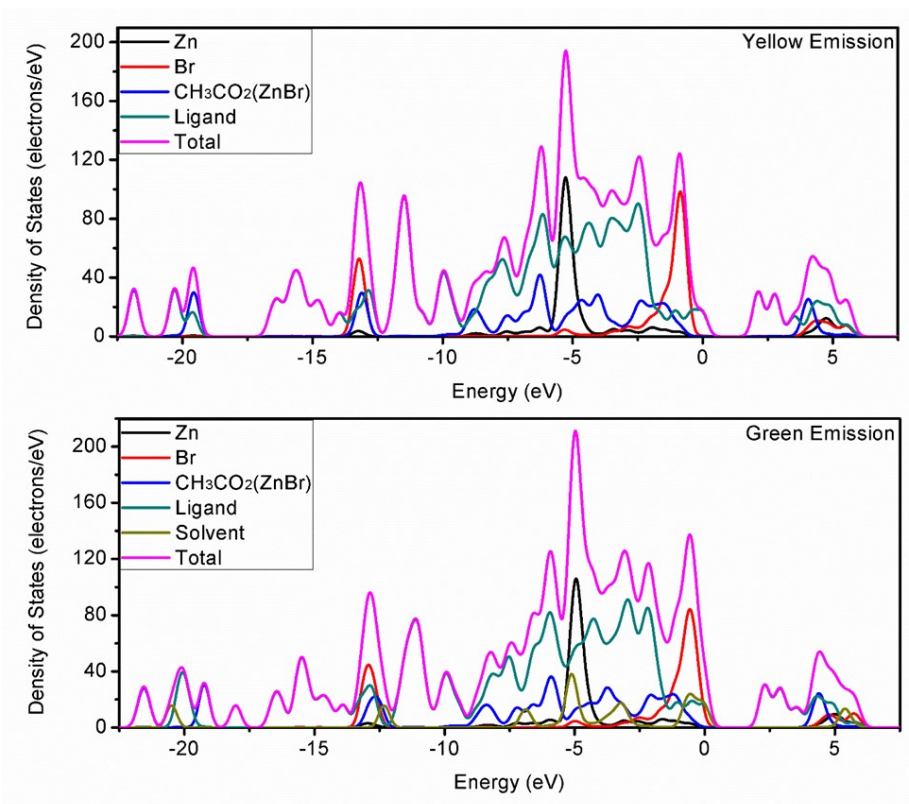


Figure S9. Density of states (DOS) of complexes 1 and 2

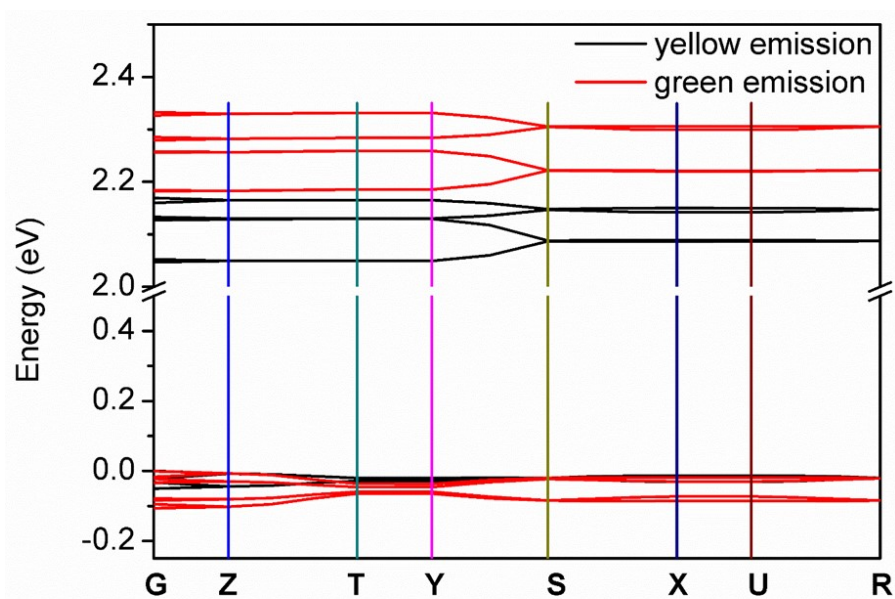


Figure S10. Band structure of complexes 1 and 2

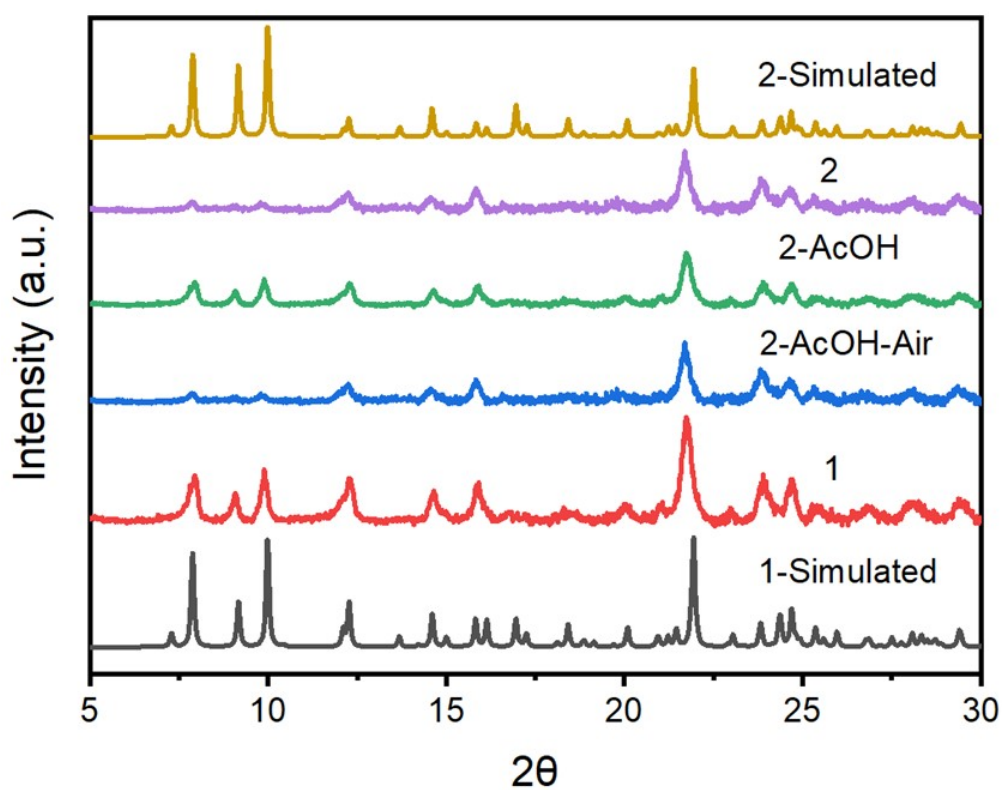


Figure S11. The PXRD patterns of 2 upon AcOH uptake (2-AcOH), AcOH release (2-AcOH-Air) and 1 in a vaporchromic cycle.

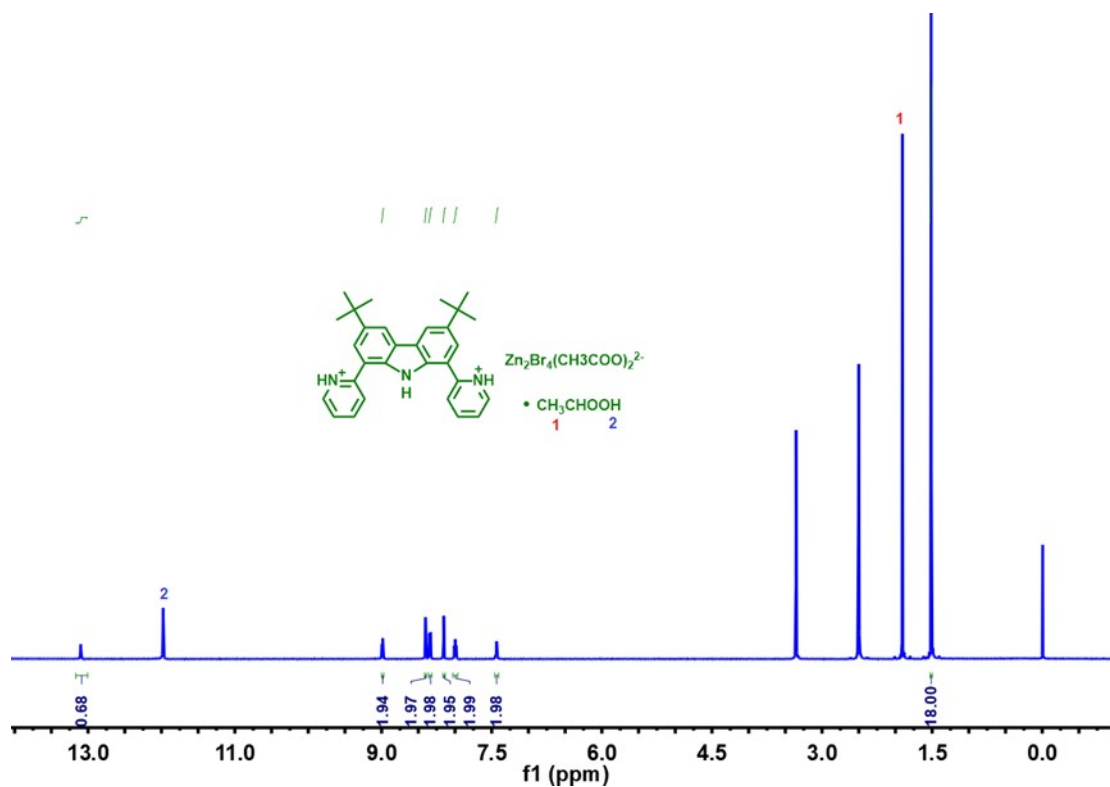


Figure S12.  $^1\text{H}$  NMR spectrum of complex 2 exposed in acetic acid atmosphere.

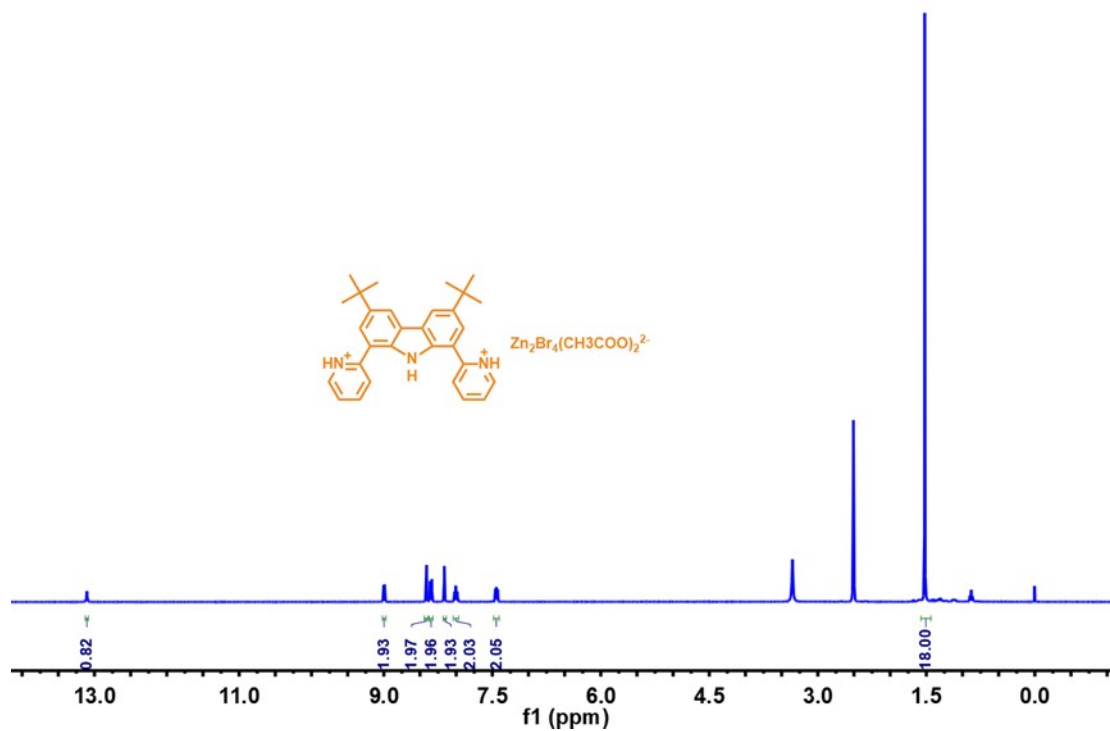


Figure S13.  $^1\text{H}$  NMR spectrum of complex 2.

Reference:

1. S. J. Clark, M. D. Segall, C. J. Pickard, P. J. Hasnip, M. J. Probert, K. Refson, M. C. Payne, *Z. Kristallogr.* 2005, 220, 567-570.
2. K. Refson, S. J. Clark, P. R. Tulip, *Phys. Rev. B* 2006, 73, 155114-155112.
3. J. P. Perdew, K. Burke, M. Ernzerhof, *Phys. Rev. Lett.* 1996, 77, 3865-3868.